Original Article

LncRNA NEAT1-miR-101-3p/miR-335-5p/miR-374a-3p/miR-628-5p-TRIM6 axis identified as the prognostic biomarker for lung adenocarcinoma via bioinformatics and meta-analysis

Dong-Xiao Ding[1#], Qiao Li[2#], Ke Shi[1], Hui Li[3], Qiang Guo[2,4], Yun-Qiang Zhang[1]

[1]Department of Thoracic Surgery, Beilun District People's Hospital of Ningbo, Ningbo, China; [2]Department of Thoracic Surgery, Affiliated Hospital of Zunyi Medical University, Zunyi, China; [3]Women and Children's Hospital of Ningbo, Ningbo, China; [4]Department of Cardiothoracic Surgery, Taihe Hospital, Hubei University of Medicine, Shiyan, China

Contributions: (I) Conception and design: YQ Zhang, Q Guo; (II) Administrative support: DX Ding, YQ Zhang; (III) Provision of study materials or patients: Q Guo, K Shi, H Li; (IV) Collection and assembly of data: Q Li, Q Guo; (V) Data analysis and interpretation: DX Ding, Q Li, Q Guo; (VI) Manuscript writing: All authors; (VII) Final approval of manuscript: All authors.

[#]These authors contributed equally to this work.

Correspondence to: Yun-Qiang Zhang. Department of Thoracic Surgery, Beilun District People's Hospital of Ningbo, Ningbo, China. Email: yunqiangzhang2021@163.com; Qiang Guo. Department of Thoracic Surgery, Affiliated Hospital of Zunyi Medical University, Zunyi, China; Department of Cardiothoracic Surgery, Taihe Hospital, Hubei University of Medicine, Shiyan, China. Email: guoqianglidan@163.com.

Background: Overexpression of the tripartite motif containing 6 (TRIM6) is associated with dismal prognosis in cancer patients, but its exact roles in lung adenocarcinoma (LUAD) have not been reported.

Methods: The roles of TRIM6 are identified by using The Cancer Genome Atlas (TCGA), TIMER2, Gene Expression Omnibus (GEO), etc., and the regulatory networks and related-prognostic biomarkers of TRIM6 are identified via the ENCORI and LNCAR databases in the LUAD progression.

Results: TRIM6 expression level in LUAD tissues was significantly increased. TRIM6 over-expression level in LUAD patients was associated with smoking, clinical stage, histological type, lymph node metastasis, TP53 mutation and dismal prognosis, and related to prognosis-related age, race, sex, clinical stage and tumor purity of LUAD patients. TRIM6 overexpression was associated with the levels of $CD8^+$ T cells, macrophages, neutrophils and myeloid dendritic cells, and correlated with the levels of LUAD immune cell markers CD8A, IRF5, CD163, VSIG4, MS4A4A, ITGAM, HLA-DPA1, NRP1, ITGAX, etc. TRIM6 might influence the progression of LUAD by regulating homologous recombination, oocyte meiosis, and ubiquitin-mediated proteolysis. LUAD patients with overexpression of miR-101-3p, miR-335-5p, miR-374a-3p, miR-628-5p, and NEAT1 had a poor prognosis.

Conclusions: NEAT1-miR-101-3p/335-5p/374a-3p/628-5p-TRIM6 network, which we constructed from our results, might be an important factor in the dismal prognosis of LUAD patients.

Keywords: NEAT1; overall survival (OS); disease-free survival (DFS); lung adenocarcinoma (LUAD); tripartite motif containing 6 (TRIM6)

Submitted Sep 10, 2021. Accepted for publication Oct 29, 2021.
doi: 10.21037/tcr-21-2181
View this article at: https://dx.doi.org/10.21037/tcr-21-2181

Introduction

New cases of lung cancer (LC) are a high proportion of the total number of cancers globally, and the mortality rate is high (1,2). In recent years, there have been some novel molecules expected to delay the progression of LC and improve the prognosis of patients (3-6). For example, atezolizumab is a monoclonal antibody that binds to programmed death-ligand 1 (PD-L1) and blocks the interaction between PD-L1 and the programmed cell death-1 (PD-1) and B7.1 receptor. Compared with chemotherapy alone, combination therapy of atezolizumab and chemotherapy has been more effective in patients with advanced non-small cell lung cancer (NSCLC), with improved overall survival (OS) (3). In pStage IA1–IB high-malignant subtype and Stage IIA–IIIA patients, epidermal growth factor receptor (EGFR)-positive patients have worse 5-year recurrence-free survival (RFS) than EGFR-negative patients. Positive EGFR mutation status is significantly related to the patient's RFS (4). However, there is still a need to identify more valuable biomarkers to extend OS for cancer patients.

During the development of NSCLC, some molecules are often expressed abnormally, including genes, micro RNAs (miRNAs), long non-coding RNAs (lncRNAs), etc. (7-11). For example, lncRNA TRPM2-AS is overexpressed in NSCLC tissues and cells. The proliferation, migration and invasive ability of NSCLC cells that interfered with the expression of TRPM2-AS were inhibited, and apoptosis was significantly increased. TRPM2-AS increases the expression level of EGFR by regulating the expression of sponge miR-138-3p, thereby promoting the proliferation, migration and invasion of NSCLC cells, and aggravating tumor growth and migration (7). lncRNA LCAT1 is significantly upregulated in LC tissues and associated with a dismal prognosis. Interfering with LCAT1 expression inhibits the growth and invasion of LC cells and tumor development in nude mice both *in vitro* and *in vivo*. LCAT1 plays a role as the competitive endogenous RNAs (ceRNAs) of miR-4715-5p, which leads to the upregulation of RAC1 activity of the endogenous target RAC family. Inhibitory effects on the expression of RAC1 improved the efficacy of paclitaxel monotherapy against LC cells *in vitro* (11). The expression levels of lncRNA DNAH17-AS1 and CCNA2 were significantly upregulated in NSCLC tissues and cells, while the expression level of miR-877-5p was significantly decreased. Overexpression of DNAH17-AS1 is associated with the TNM stage, distant metastasis, short OS, and disease-free survival (DFS) of NSCLC patients. Interfering with the expression of DNAH17-AS1 inhibits the proliferation, migration and invasion of NSCLC cells, and promotes cell apoptosis. DNAH17-AS1 could upregulate CCNA2 to played a carcinogenic role by acting as a sponge for miR-877-5p (12). These results suggest that the ceRNA network plays an important role in delaying the progression of NSCLC.

The tripartite motif containing 6 (TRIM6) also plays a crucial role in carcinogenesis (13-15). It is upregulated in colorectal cancer (CRC) and its expression level is an independent predictor of dismal prognosis in CRC patients. Knocking down TRIM6 expression inhibits the proliferation and cell cycle arrest of CRC cells, and increases the sensitivity of cells to 5-fluorouracil and oxaliplatin. TRIM6 promotes CRC progression through the TiS21/FOXM1 mechanism (13), and its expression level is significantly enhanced in breast cancer (BC) cells and tissues. Overexpression of TRIM6 promotes BC progression by increasing YAP1, while knocking out TRIM6 has the opposite effect. TRIM6 promotes ubiquitination-mediated STUB1 degradation to promote YAP1 signaling transduction. Overexpression of STUB1 reduces the promoting effect of TRIM6 on BC cell growth (10). However, the roles of TRIM6 in the progression of NSCLC and its adenocarcinoma (LUAD) subtypes has not been reported. Therefore, the roles of and potential mechanisms of TRIM6 in the progression of LUAD were comprehensively analyzed in this study based on The Cancer Genome Atlas (TCGA), TIMER2, and Gene Expression Omnibus (GEO) databases, and the upstream regulatory network of TRIM6 was constructed to provide new candidate prognostic biomarkers for the treatment of LUAD patients. We present the following article in accordance with the REMARK reporting checklist (available at https://dx.doi.org/10.21037/tcr-21-2181).

Methods

The study was conducted in accordance with the Declaration of Helsinki (as revised in 2013).

TCGA database

Gene expression of 594 LUAD FKPM and 522 clinical data were downloaded from the TCGA database, and TRIM6 expression data were extracted for analysis in LUAD tissues. In the analysis of TRIM6 expression and survival of NSCLC patients, patients with missing prognostic information were excluded.

GEO database

The series matrix data files for the GSE1037, GSE18842, GSE19188 and GSE30219 datasets were downloaded from the GEO database website. GSE1037 dataset platform was GPL962: CHUGAI 41K. The platform of GSE18842, GSE19188 and GSE30219 datasets was GPL570: [HG-U133_PLUS_2] Affymetrix Human Genome U133 Plus 2.0 Array.

UALCAN database

The UALCAN database was used to analyze the cancer gene expression level and patient prognosis or clinicopathological characteristics of LUAD patients. TRIM6 expression level and the clinical values of TRIM6 in LUAD were investigated using the UALCAN database.

Lung cancer explorer (LCE) database

The LCE database, which includes multicenter data, was used to show the relationship between gene expression and survival in LC patients. In this database, the TRIM6 expression level and its prognostic value in LUAD were demonstrated by meta-analysis.

GEPIA2 database

This is a secondary database developed in recent years based on cancer gene expression data from the TCGA and GTEX databases. The GEPIA2 website has the advantage of being simple to operate and can be used to investigate the TRIM6 expression in cancer tissues and its value in the OS and DFS of LUAD patients.

TIMER2 database

The TIMER2 database displays gene expression levels in pan-cancer tissue by using cancer data from the TCGA database, and identifies the relationship between gene expression level and cancer immune purity, immune cells and cell markers. The TRIM6 expression level in pan-cancer tissues and its potential value in immunity and prognosis were analyzed.

Creation of lncRNA-miRNA-gene network

The upstream binding miRNAs of TRIM6 and miRNA-binding lncRNAs were screened in the ENCORI database. The expression of TRIM6-binding miRNAs in LUAD tissues and the role in prognosis were verified in miRNA expression level and prognosis module, and the clinical value of miRNA-binding lncRNAs was identified in the LNCAR database and literature reports. In our study, the value of NEAT1 in the prognosis of LUAD patients was explored using meta-analysis of the literature in recent years. From this, a lncRNA-miRNA-gene network was constructed.

Meta-analysis

A systematic search from 6 relevant databases including PubMed, Embase, Cochrane Library, Web of Science, Google Scholar and CNKI was executed to get all related papers. The software of Review Manager 5.3 was applied to analyze the prognostic data. HRs with 95% CI were used to inquiry the correlation between aberrant NEAT1 expression and the OS via meta-analysis (16).

TRIM6-related signaling pathways

In 539 LUAD tissues, the median expression value of TRIM6 was grouped, and gene set enrichment analysis (GSEA) was conducted to investigate the potential mechanisms of high and low TRIM6 expression in LUAD progression (2). The model was run 1,000 times in GSEA software.

Statistical analysis

The mean levels of TRIM6 and NEAT1 in LUAD tissues were determined by *t* test. The relationship between TRIM6 expression level and the survival time of LUAD patients was assessed via the survival analysis. $P<0.05$ was considered statistically significant.

Results

Expression of TRIM6 in pan-cancer tissues

In the TIMER2 database, TRIM6 was overexpressed in cholangiocarcinoma, esophageal carcinoma, glioblastoma multiforme, liver hepatocellular carcinoma and LUAD tissues, and was under-expressed significantly in breast invasive carcinoma, colon adenocarcinoma, head and neck squamous cell carcinoma, kidney chromophobe, kidney renal

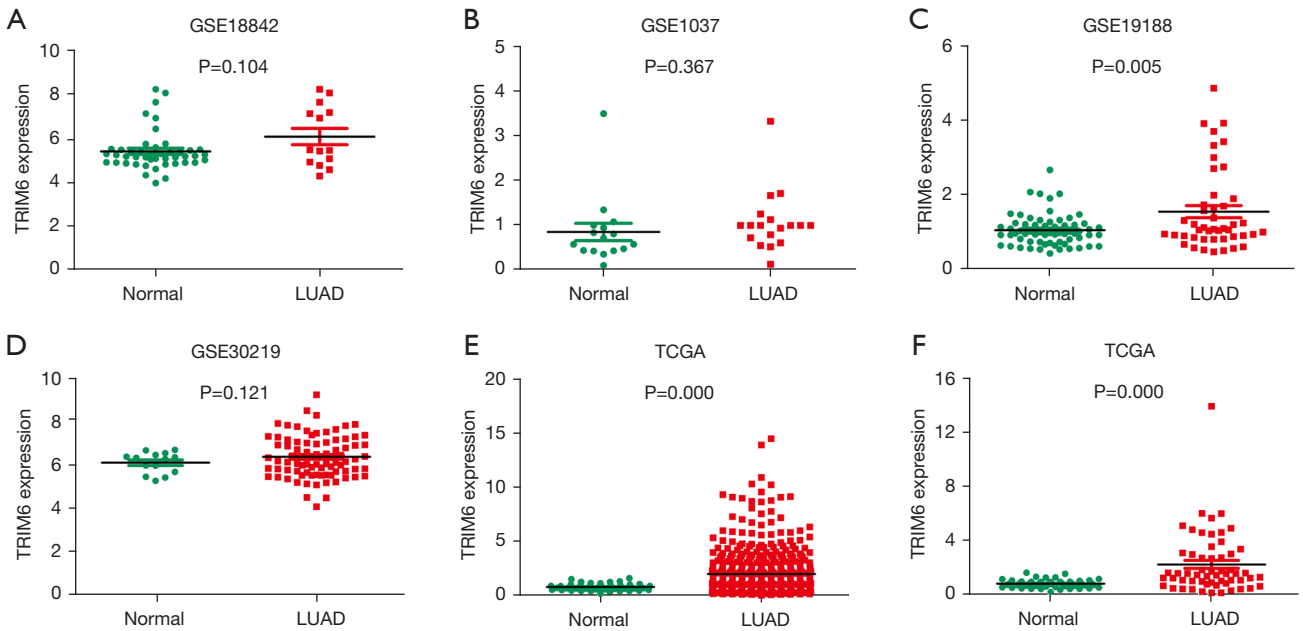

Figure 1 TRIM6 expression level significantly increased in LUAD tissues. (A-D) GSE18842, GSE1037, GSE19188, and GSE30219 datasets; (E,F) unpaired and paired LUAD tissues in TCGA database. TRIM6, tripartite motif containing 6; LUAD, lung adenocarcinoma. TCGA, The Cancer Genome Atlas.

clear cell carcinoma, kidney renal papillary cell carcinoma, prostate adenocarcinoma, rectal adenocarcinoma and uterine corpus endometrial carcinoma tissues (Figure S1).

Overexpression of TRIM6 in LUAD tissues

In the TCGA and GEO databases, the TRIM6 expression level was significantly increased in LUAD tissues. The GSE18842, GSE1037, GSE19188, and GSE30219 datasets showed TRIM6 overexpression in LUAD tissues. The result for the GSE19188 dataset was statistically significant (*Figure 1A-1D*). In the TCGA database, TRIM6 was overexpressed in unpaired LUAD tissues (*Figure 1E*), and in 59 paired LUAD tissues (*Figure 1F*). Meta-analysis of the data from TCGA and GEO databases revealed that TRIM6 was overexpressed in LUAD tissues (Figure S2).

Relation of TRIM6 expression level to smoking, clinical stage, histological type, lymph node metastasis and TP53 mutation in LUAD patients

In the UALCAN database, the TRIM6 expression level was associated with smoking, clinical stage, histological type, lymph node metastasis and TP53 mutation in LUAD patients according to correlation analysis (*Figure 2*). TRIM6 expression level was related to smoking (Nonsmoker *vs.* Reformed smoker 2, P=1.173520E-02), clinical stage (Stage 1 *vs.* Stage 2, P=8.863900E-03; Stage 1 *vs.* Stage 3, P=3.498400E-03), histological type (Not Otherwise Specified, NOS) *vs.* Papillary, P=4.411700E-02), lymph node metastasis (N0 *vs.* N2, P=4.879600E-03), and TP53 mutation (TP53-Mutant *vs.* TP53-NonMutant, P=4.360600E-04) in LUAD patients. In the TIMER2 database, TRIM6 expression showed statistical significance in both the wild type and mutant type (Figure S3).

Overexpression of TRIM6 and dismal prognosis in LUAD patients

Survival analysis showed that TRIM6 overexpression was associated with poor prognosis in patients with LUAD (*Figure 3* and Figure S3). In the TCGA database, TRIM6 overexpression was associated with shorter OS in LUAD patients compared with the group with lower TRIM6 expression (*Figure 3A*). In the GEPIA2 database, TRIM6 overexpression was associated with shorter OS and DFS in LUAD patients compared with the group with low TRIM6 expression (*Figure 3B,3C*). Meta-analysis

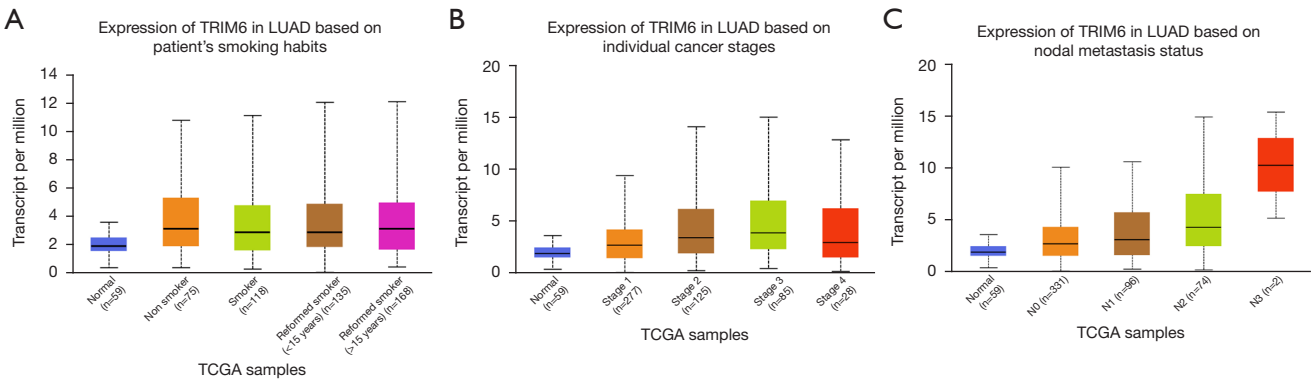

Figure 2 Association of TRIM6 expression level with (A) smoking, (B) clinical stage, and (C) lymph node metastasis of LUAD patients. TRIM6, tripartite motif containing 6; LUAD, lung adenocarcinoma; TCGA, The Cancer Genome Atlas.

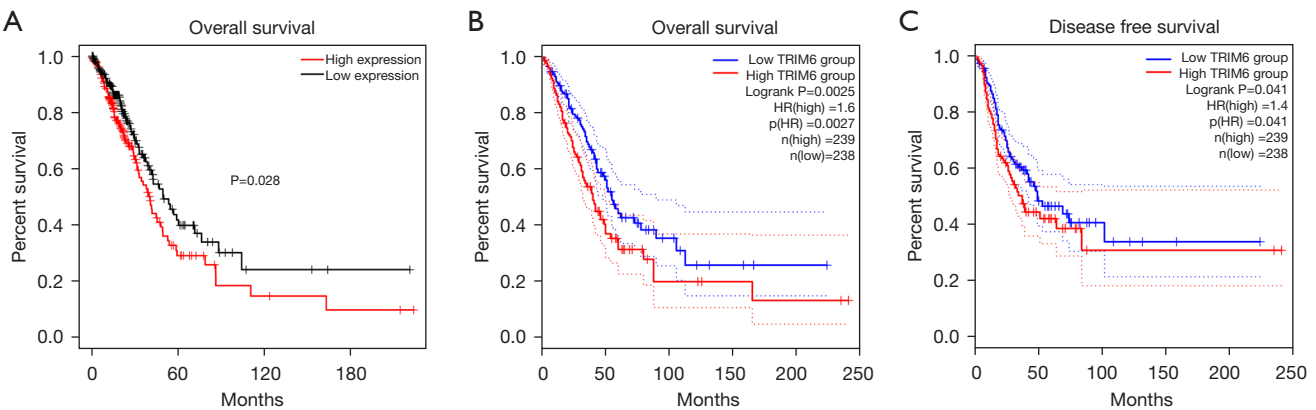

Figure 3 Correlation of TRIM6 overexpression level with LUAD short overall survival (A,B) and disease-free survival (C). TRIM6, tripartite motif containing 6; LUAD, lung adenocarcinoma.

of the data from TCGA and GEO databases revealed that TRIM6 overexpression was a risk factor for poor prognosis in LUAD patients (Figure S4).

Correlation of overexpression of TRIM6 with prognosis-related age, race, sex, clinical stage, and tumor purity in LUAD patients

TRIM6 overexpression was associated with prognosis-related age, race, sex, clinical stage, and tumor purity in LUAD patients in the survival analysis (*Figure 4*). In the TIMER2 database, TRIM6 overexpression was associated with dismal prognosis in LUAD patients (*Figure 4A*). TRIM6 overexpression was associated with prognosis-related tumor purity, age, race, sex, and clinical stage in LUAD patients via subgroup analysis (*Figure 4B-4F*).

Relation of TRIM6 overexpression to levels of CD8$^+$ T cells, macrophages, neutrophils and myeloid dendritic cells

In the TIMER2 database, the TRIM6 overexpression level was related to the levels of CD8$^+$ T cells, macrophages, neutrophils and myeloid dendritic cells (*Table 1*). In the LUAD tissues of the GEPIA2 database, the TRIM6 expression level correlated with the levels of LUAD immune cell markers IRF5 (r=0.21), CD163 (r=0.2), VSIG4 (r=0.2), MS4A4A (r=0.18), ITGAM (r=0.23), HLA-DPB1 (r=0.11), HLA-DRA (r=0.13), HLA-DPA1 (r=0.16), NRP1 (r=0.29), and ITGAX (r=0.16), all of which were statistically significant (*Figure 5*, *Table 2*). In the ENCORI database, the TRIM6 expression level correlated with the levels of LUAD immune cell markers CD8A (r=0.106), IRF5 (r=0.143), CD163 (r=0.15), VSIG4 (r=0.123), MS4A4A (r=0.124),

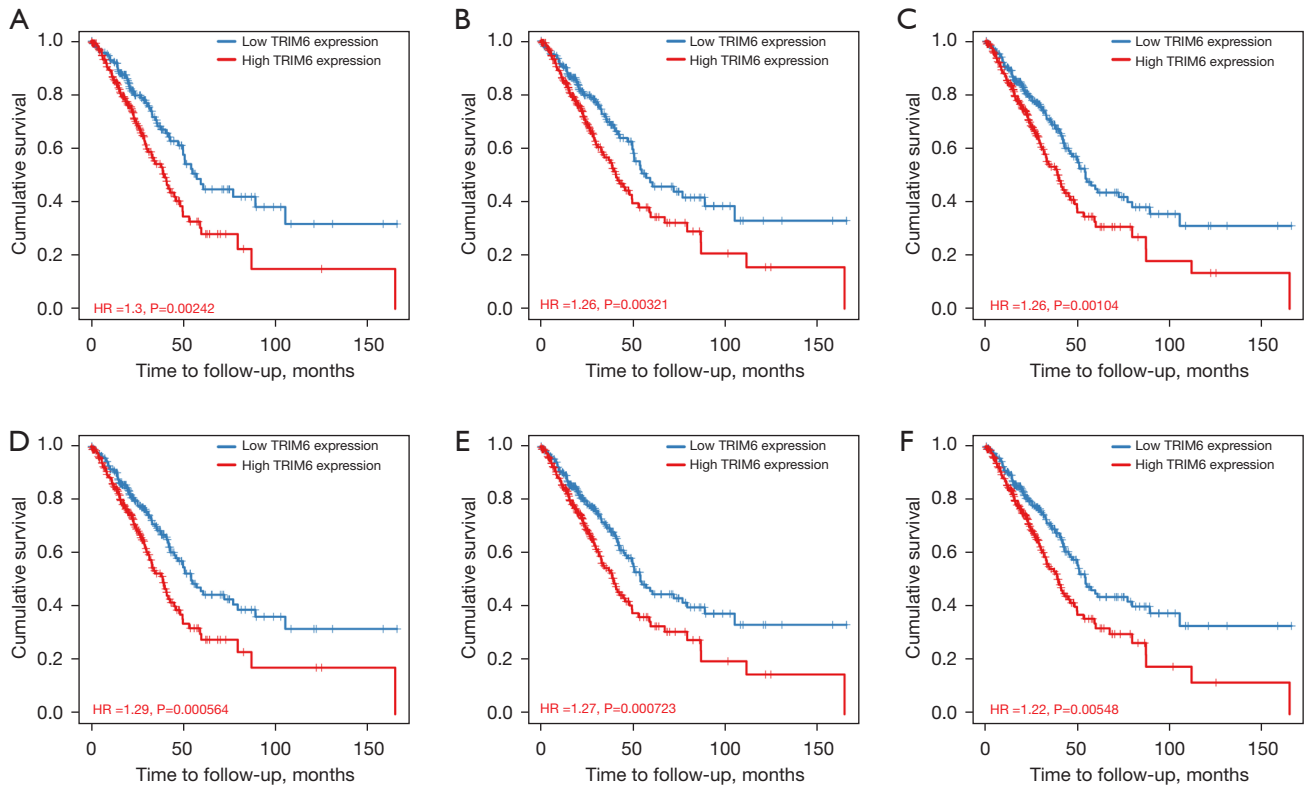

Figure 4 Association of TRIM6 overexpression level with dismal prognosis, age, race, sex, clinical stage, and tumor purity in LUAD patients. (A) Overall survival; (B-F) tumor purity, age, race, sex, and clinical stage. TRIM6, tripartite motif containing 6; LUAD, lung adenocarcinoma.

Table 1 Relationship of TRIM6 overexpression to the immune cells of LUAD

Infiltrate	r	P	Adjusted P
$CD8^+$ T cells	0.226788294	3.60E-07	8.99E-06
Neutrophils	0.163253153	0.000272579	0.001447699
Macrophages	0.133174932	0.003049891	0.009530909
Myeloid dendritic cells	0.180194277	5.73E-05	0.000584439

TRIM6, tripartite motif containing 6; LUAD, lung adenocarcinoma.

ITGAM (r=0.135), HLA-DPA1 (r=0.107), NRP1 (r=0.178) and ITGAX (r=0.107), and all were statistically significant (*Figure 6*, *Table 3*).

Possible involvement of TRIM6 in the biological functions and signaling mechanisms of LUAD

The GSEA results suggested that increased TRIM6 might be involved in sister chromatid cohesion, cellular carbohydrate catabolic process, meiotic cell cycle process, positive regulation of DNA replication, DNA recombination, cytokinesis and other biological processes (Figure S5, Table S1), and participate in the regulation of homogeneous recombination, ubiquitin mediated proteolysis, mismatch repair, nucleotide excision repair, pyrimidine metabolism, RNA degradation, RIG I like receptor signaling pathway, and oocyte meiosis (*Figure 7*).

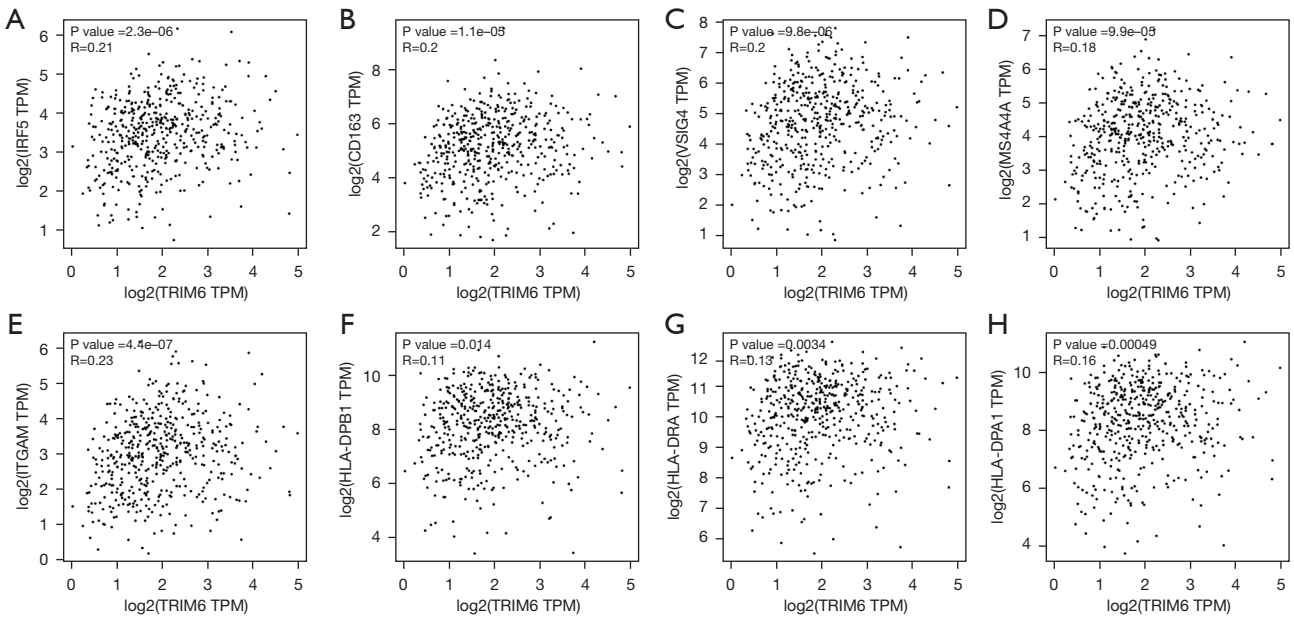

Figure 5 Correlation of TRIM6 with the levels of LUAD immune cell markers in the GEPIA2 database (A-H). TRIM6, tripartite motif containing 6; LUAD, lung adenocarcinoma.

Table 2 Relationship of TRIM6 overexpression to the markers of immune cells in LUAD tissues from the GEPIA2 database

Cell type	Markers	r	P
$CD8^+$ T cell	CD8A	0.089	0.051
	CD8B	–0.02	0.67
Macrophage	INOS (NOS2)	0.049	0.28
	IRF5	0.21	2.3e-06
	COX2 (PTGS2)	0.08	0.079
	CD163	0.2	1.1e-05
	VSIG4	0.2	9.8e-06
	MS4A4A	0.18	9.9e-05
Neutrophil	CD66b (CEACAM8)	0.081	0.075
	CD11b (ITGAM)	0.23	4.4e-07
Dendritic cell	HLA-DPB1	0.11	0.014
	HLA-DQB1	0.063	0.17
	HLA-DRA	0.13	0.0034
	HLA-DPA1	0.16	0.00049
	BDCA-1 (CD1C)	0.033	0.47
	BDCA-4 (NRP1)	0.29	4.7e-11
	CD11c (ITGAX)	0.16	0.00045

TRIM6, tripartite motif containing 6; LUAD, lung adenocarcinoma.

NEAT1-miRNAs-TRIM6 network

In the ENCORI database, the miRNAs that TRIM6 bound were miR-23a-3p, miR-25-3p, miR-32-5p, miR-33a-5p, miR-92A-3p, miR-101-3p, miR-196a-5p, miR-219a-5p, miR-23b-3p, and miR-137, miR-142-3p, miR-146a-5p, miR-361-5p, miR-363-3p, miR-376c-3p, miR-379-5p, miR-381-3p, miR-383-5p, miR-337-3p, miR-335-5p, miR-196b-5p, miR-146b-5p, miR-495-3p, miR-524-5p, miR-520d-5p, miR-520g-3p, miR-520h, miR-508-3p, miR-92b-3p, miR-33b-5p, miR-641, miR-542-3p, miR-758-3p, miR-374a-3p, miR-628-5p, miR-300, miR-513c-5p, miR-1321, miR-2115-3p, miR-514b-5p and miR-5688. miR-513c-5p, miR-514b-5p, miR-25-3p, miR-376c-3p, miR-520d-5p, miR-196b-5p, miR-337-3p, miR-146a-5p, miR-374a-3p, miR-137, MIR-101-3p, miR-146b-5p, miR-32-5p, miR-758-3p, miR-542-3p, miR-628-5p, miR-196a-5p, miR-33a-5p, miR-219a-5p, miR-335-5p, miR-33b-5p, and miR-142-3p, which were all overexpressed in LUAD tissues ($P<0.05$). miR-520G-3p, miR-524-5p, miR-383-5p, and miR-520h showed low expression in LUAD tissues ($P<0.05$, *Figure 8*).

In addition, the role of miRNAs in the prognosis of LUAD patients was analyzed by survival analysis, and the results showed that LUAD patients with overexpression of miR-101-3p, miR-335-5p, miR-374a-3p and miR-628-5p had a poor prognosis, with statistical significance (*Figure 9*).

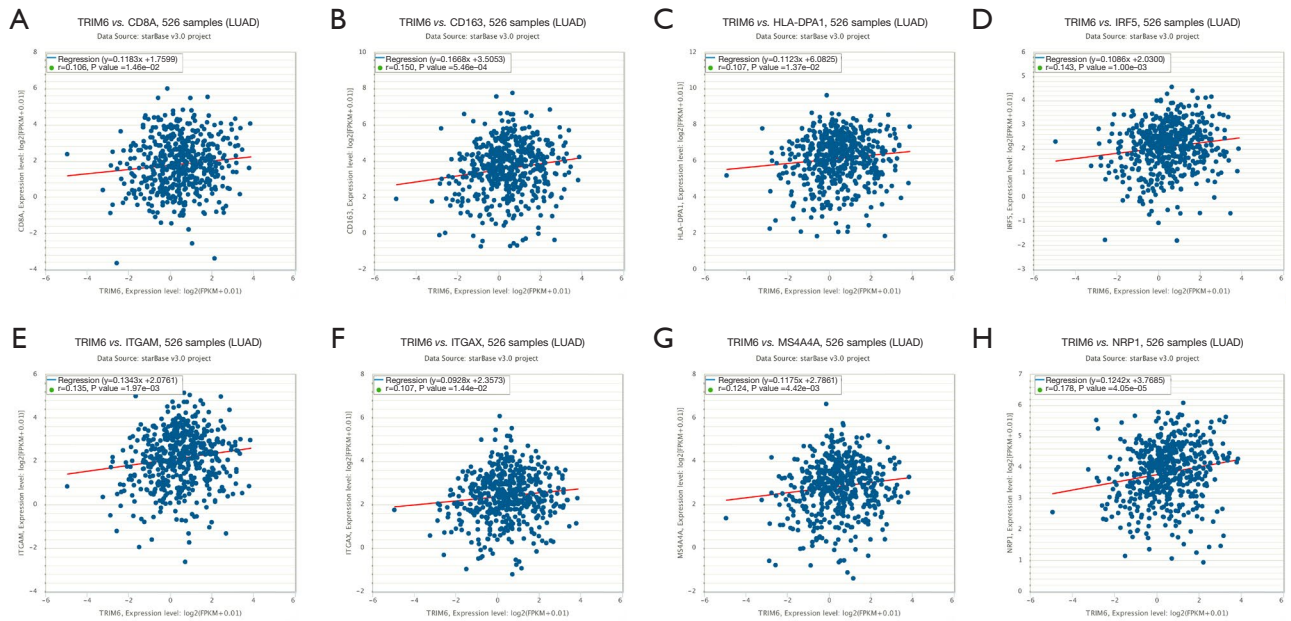

Figure 6 Correlation of TRIM6 with the levels of LUAD immune cell markers in the ENCORI database (A-H). TRIM6, tripartite motif containing 6; LUAD, lung adenocarcinoma.

Table 3 Relationship of TRIM6 overexpression to the markers of immune cells in LUAD tissues from the ENCORI database

Cell type	Markers	r	p
$CD8^+$ T cell	CD8A	0.106	0.0146
	CD8B	0.006	0.9
Macrophage	INOS (NOS2)	–0.024	0.582
	IRF5	0.143	0.001
	COX2 (PTGS2)	0.041	0.348
	CD163	0.15	5.46e-4
	VSIG4	0.123	4.81e-3
	MS4A4A	0.124	4.42e-3
Neutrophil	CD66b (CEACAM8)	0.039	0.372
	CD11b (ITGAM)	0.135	1.97e-03
Dendritic cell	HLA-DPB1	0.05	0.254
	HLA-DQB1	0.052	0.23
	HLA-DRA	0.084	0.0545
	HLA-DPA1	0.107	0.0137
	BDCA-1 (CD1C)	–0.024	0.577
	BDCA-4 (NRP1)	0.178	4.05e-5
	CD11c (ITGAX)	0.107	0.0144

TRIM6, tripartite motif containing 6; LUAD, lung adenocarcinoma.

It was found that lncRNA NEAT1 might regulate miR-101-3p, miR-335-5p, miR-374a-3p and miR-628-5p through MRE via the miRNA–23), and NEAT1 (LC_S257) was overexpressed in LUAD tissues in the LNCAR database. The expression levels of NEAT1 (LC_S149) and NEAT1 (LC_S216) in LUAD tissues were significantly decreased (*Figure 10*). *Figure 11* shows that NEAT1 overexpression in LUAD tissues was related to dismal prognosis of LUAD patients via meta-analysis (14-19). The constructed TRIM6 network mechanism provides a new regulatory mechanism for LUAD progression (Figure S6).

Discussion

In recent years, more and more studies have reported the involvement of ceRNA networks in regulating the progression of LUAD (17-19). Compared with adjacent normal tissues, LINC00942 is up-regulated in LUAD tissues. Overexpression of LINC00942 is associated with dismal survival. Low expression of LINC00942 inhibits the proliferation, migration and invasion of A549 and H1299 cells, and promotes cell apoptosis. LINC00942 up-regulates the expression of FZD1 by combining miR-5006-5p to participate in the growth and migration of LUAD (17). circ-AASDH is highly expressed in LUAD

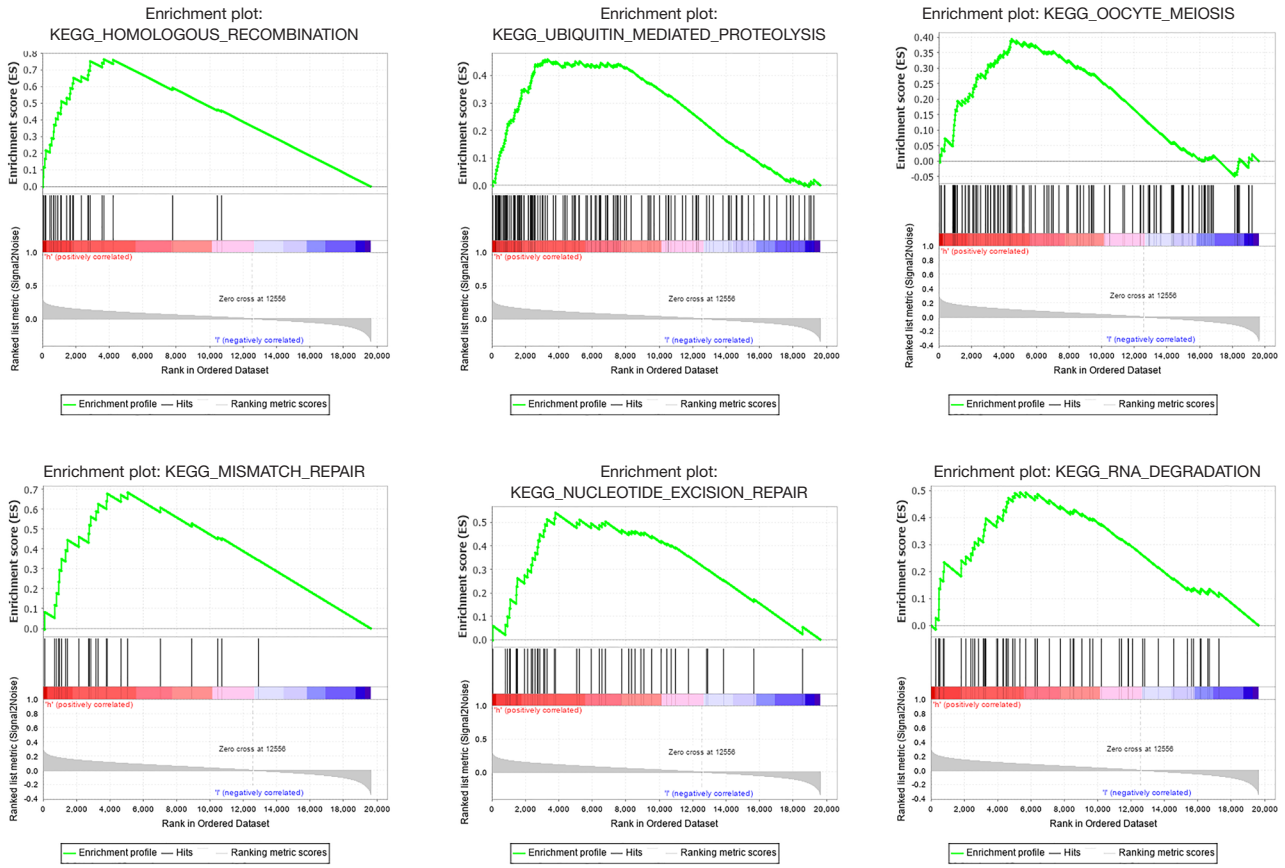

Figure 7 Possible involvement of TRIM6 in the signaling mechanisms of LUAD via gene set enrichment analysis. TRIM6, tripartite motif containing 6; LUAD, lung adenocarcinoma.

tissues and cells, and is related to tumor size, clinical stage and dismal prognosis. Interfering with the expression of circ-AASDH can inhibit the proliferation and migration of LUAD cells and promote cell apoptosis. circ-AASDH can act as a sponge of miR-140-3p to promote E2F7 expression (19). In this study, we found that TRIM6 was excessively elevated in LUAD tissues from a multi-database analysis. TRIM6 overexpression was associated with smoking, clinical stage, histological type, lymph node metastasis, TP53 mutation, and dismal prognosis in LUAD patients, and was associated with prognosis-related age, race, sex, clinical stage, and tumor purity in LUAD patients. We constructed the NEAT1-miR-101-3p/miR-335-5p/miR-374a-3p/miR-628-5p-TRIM6 signaling axis, which is related to LUAD progression. Recent multicenter data suggest that NEAT1 acts as an oncogenic factor in NSCLC progression (20-25). NEAT1 is highly expressed in NSCLC tissues and cells, and closely associated with advanced clinical stage, lymph node metastasis, distant metastasis, and dismal prognosis in NSCLC patients (25,26). Knocking down NEAT1 expression inhibits NSCLC and LUAD cell growth and migration (26,27). NEAT1 is highly expressed in LUAD tissues. NEAT1 overexpression is related to the late TNM stage, lymph node metastasis and OS in LUAD patients, and is a risk factor for dismal prognosis in LUAD patients. Knockout of NEAT1 expression in LUAD A549 and H1299 cells can delay tumor cell proliferation and migration (21). NEAT1 is associated with drug resistance in NSCLC patients (28-30). Compared with NSCLC cells and normal bronchial epithelial cells, NEAT1 was overexpressed in paclitaxel-resistant NSCLC cells (28). Elimination of NEAT1 reversed paclitaxel resistance by increasing PARP and caspase-3 expression and inducing apoptosis, and was associated with activation of the Akt/mTOR resistance signaling pathway (29). Sorafenib treatment of A549 cells and PC9 cells reduced cell proliferation and induced cell

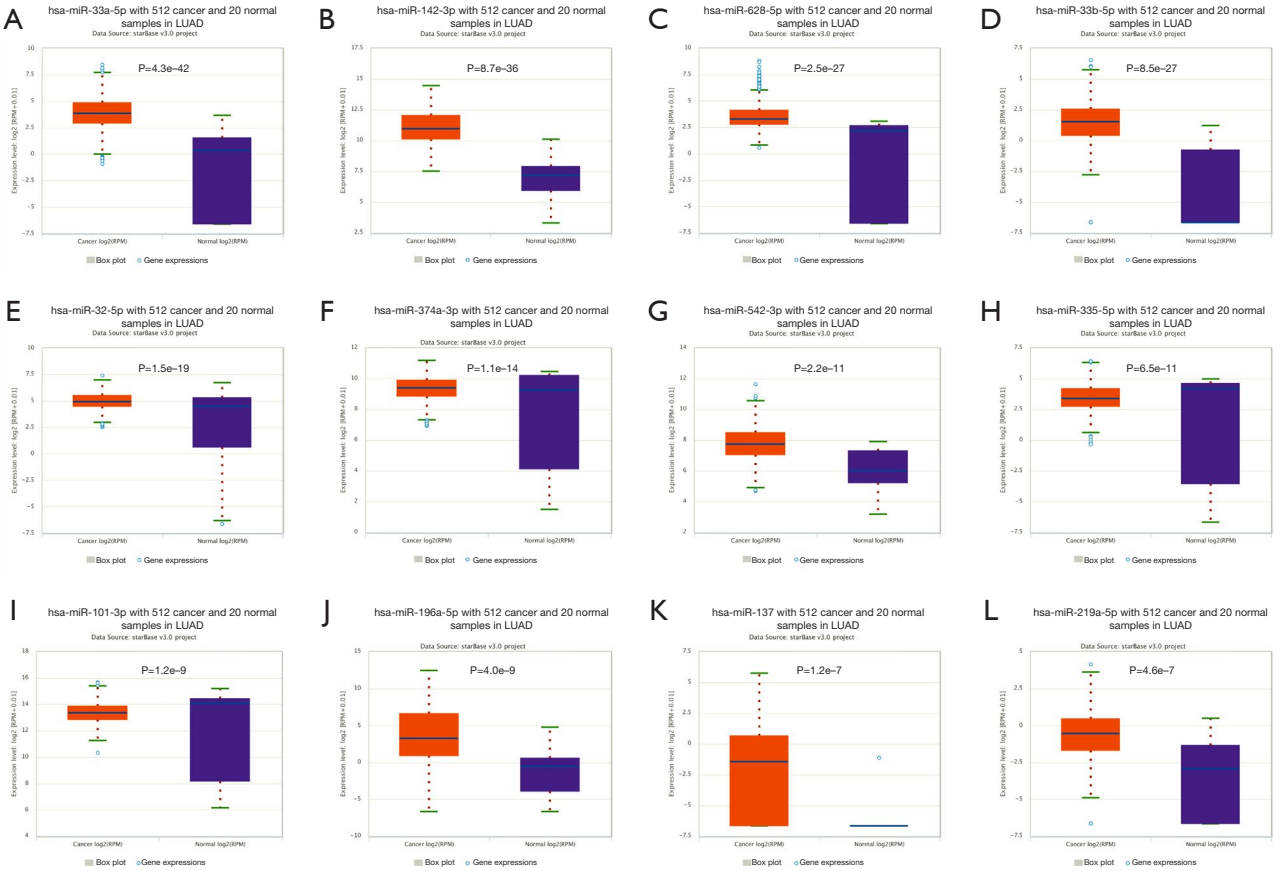

Figure 8 Abnormal expression of the microRNAs that TRIM6 bound in LUAD tissues from the ENCORI database. LUAD, lung adenocarcinoma; TRIM6, tripartite motif containing 6; LUAD, lung adenocarcinoma.

apoptosis, and the proliferation effect of NEAT1 silencing was significantly increased (30).

In addition, miR-101-3p is low expressed in NSCLC cells. Overexpression of miR-101-3p can directly bind to and inhibit the expression of MALAT-1, thereby inhibiting the proliferation, migration and invasion of NSCLC cells (31). miR-335-5p is down-regulated in NSCLC tissues. Overexpression of miR-335-5p inhibits TGF-β1-mediated NSCLC migration and invasion (32). KCNMB2-AS1 silencing hinders the proliferation, migration and invasion of NSCLC cells, promotes cell apoptosis, and inhibits tumor growth in vivo. KCNMB2-AS1 acts as a sponge for endogenous miR-374a-3p to increase ROCK1 expression (33). These results indicate that our constructed network was closely related to the metastasis and drug resistance of NSCLC. However, the roles of NEAT1-miR-101-3p/miR-335-5p/miR-374a-3p/miR-628-5p-TRIM6 signaling axis in LUAD needs to be further confirmed by constructing the cell models.

It is well known that the immune microenvironment plays an important role in LUAD progression. The tumor immune microenvironment is composed of tumor cells, immune cells, mesenchymal cells and extracellular components, which are related to genetic status. SRGN is overexpressed in TTF-1 negative LUAD cells. The expression level of SRGN in LUAD is associated with the dismal prognosis. SRGN regulates the expression of PD-L1, interleukin 6, interleukin 8 and CXC motif chemokine 1 in LUAD cells, increases the migration and invasion ability of LUAD and fibroblasts, and enhances angiogenesis. SRGN can trigger the aggressive and immunosuppressive phenotype of TTF-1 negative LUAD cells (34). Our study found that TRIM6 overexpression was related to levels of $CD8^+$ T cells, macrophages, neutrophils and myeloid dendritic cells. The TRIM6 expression level correlated with the levels of LUAD immune cell markers

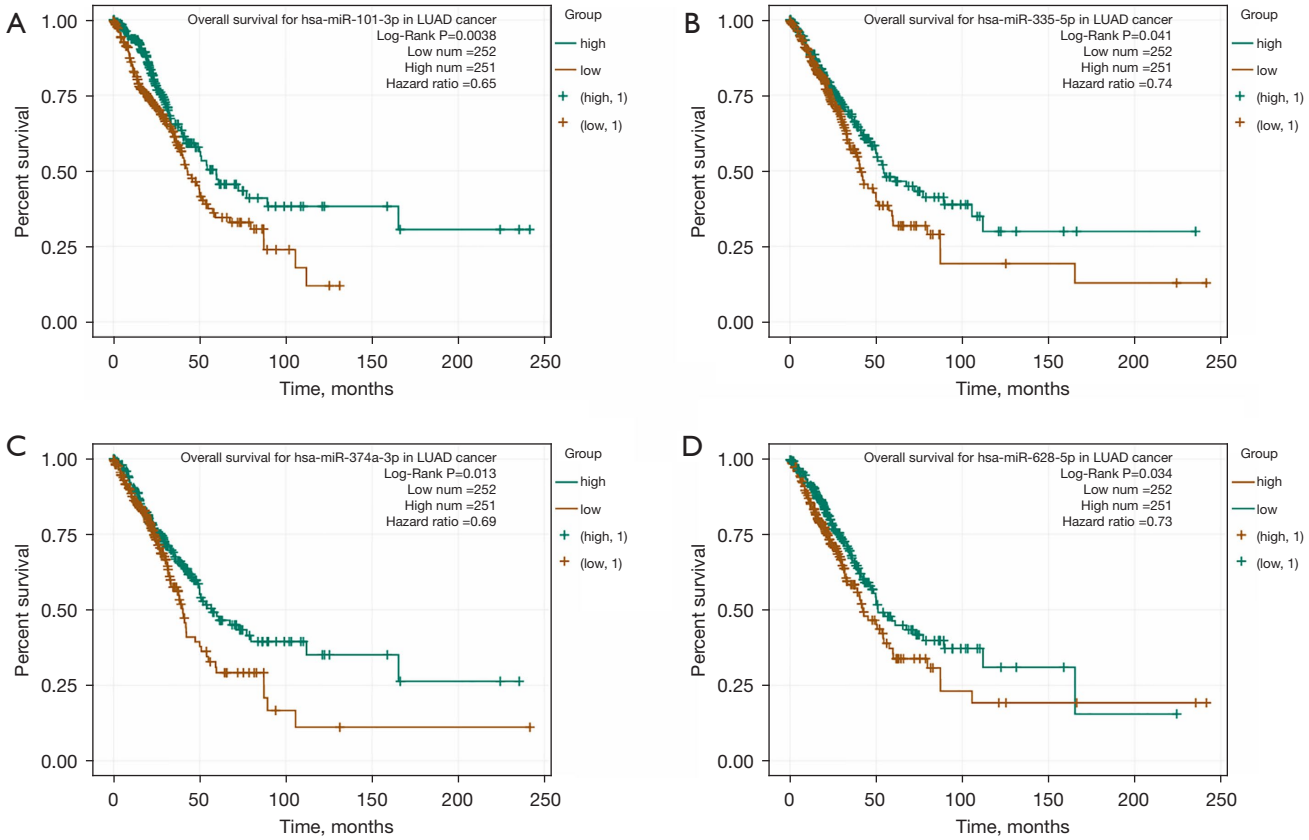

Figure 9 Dismal prognosis of LUAD patients with overexpression of (A) miR-101-3p, (B) miR-335-5p, (C) miR-374a-3p and (D) miR-628-5p. LUAD, lung adenocarcinoma.

CD8A, IRF5, CD163, VSIg4, MS4A4a, ITGAM, HLA-DPA1, NRP1 and ITGAX. CD8A is a marker of $CD8^+$ T cells; IRF5, CD163, VSIG4 and MS4A4A are markers of macrophages; ITGAM is a neutrophil marker; and HLA-DPA1, NRP1 and ITGAX are markers of dendritic cells. Studies have shown that these markers have tumor suppressor or tumor promoting effects in cancer (35-38). High CD8A expression is associated with T stage, lymph node metastasis, and prognosis in LUAD patients (35). Overexpression of CD163 in glioma specimens was associated with adverse prognosis, and loss of CD163 expression inhibited cell cycle progression and proliferation (36). CD163 silencing reduced the activity of the Akt/GSK3β/β-catenin/cyclin D1 pathway by regulating CK2 expression, but CD163 was upregulated in CD133-positive glioma stem cells (GSC) (36). Low CD163 expression resulted in altered expressions of GSC markers CD133, ALDH1A1, NANOG, and OCT4 (36). The relationship between TRIM6 and immune cells and their markers needs further confirmation.

Our study had a large sample size and utilized a variety of databases. However, it LUADked basic research demonstration, which is a future research plan.

Conclusions

TRIM6 overexpression was associated with smoking, clinical stage, histological type, lymph node metastasis, TP53 mutation, and dismal prognosis, and related to prognosis-related age, race, sex, clinical stage, and tumor purity in LUAD patients. The overexpression level of TRIM6 correlated with the levels of LUAD immune cells and their markers. NEAT1–miR-101-3p/miR-335-5p/miR-374a-3p/miR-628-5p-TRIM6 signaling network might be an important factor in the prognosis of patients with LUAD.

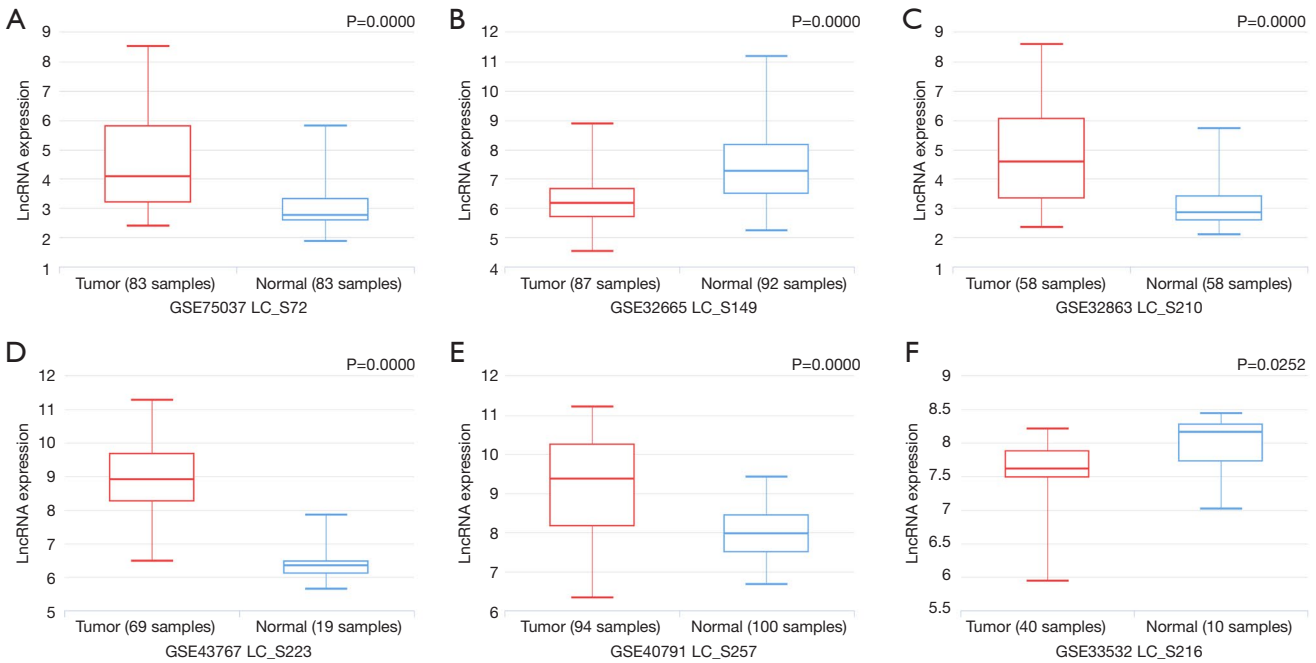

Figure 10 NEAT1 expression levels in LUAD tissues. (A) LC_S72; (B) LC_S149; (C) LC_S210; (D) LC_S223; (E) LC_S257; (F) LC_S216. LUAD, lung adenocarcinoma.

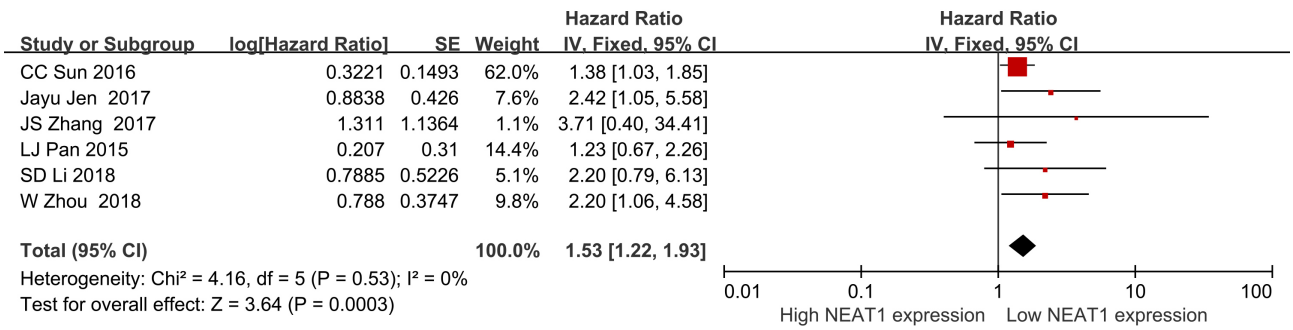

Figure 11 Relationship of NEAT1 to poor prognosis of LUAD patients via meta-analysis. LUAD, lung adenocarcinoma.

Acknowledgments

Funding: None.

Footnote

Reporting Checklist: The authors have completed the REMARK reporting checklist. Available at https://dx.doi.org/10.21037/tcr-21-2181

Conflicts of Interest: All authors have completed the ICMJE uniform disclosure form (available at https://dx.doi.org/10.21037/tcr-21-2181). The authors have no conflicts of interest to declare.

Ethical Statement: The authors are accountable for all aspects of the work in ensuring that questions related to the accuracy or integrity of any part of the work are appropriately investigated and resolved. The study was conducted in accordance with the Declaration of Helsinki (as revised in 2013).

References

1. Sung H, Ferlay J, Siegel RL, et al. Global Cancer Statistics 2020: GLOBOCAN Estimates of Incidence and Mortality Worldwide for 36 Cancers in 185 Countries. CA Cancer J Clin 2021;71:209-49.
2. Guo Q, Ke XX, Fang SX, et al. PAQR3 Inhibits Non-small Cell Lung Cancer Growth by Regulating the NF-κB/p53/Bax Axis. Front Cell Dev Biol 2020;8:581919.
3. Yamaguchi T, Hida T. Addition of atezolizumab to nab-paclitaxel plus carboplatin is a new standard option for the first-line treatment for non-squamous non-small cell lung cancer. Transl Cancer Res 2019;8:E11-4.
4. Ito M, Miyata Y, Tsutani Y, et al. Positive EGFR mutation status is a risk of recurrence in pN0-1 lung adenocarcinoma when combined with pathological stage and histological subtype: A retrospective multi-center analysis. Lung Cancer 2020; 141:107-113.
5. Kagimoto A, Tsutani Y, Izaki Y, et al. Prediction of Lymph Node Metastasis Using Semiquantitative Evaluation of PET for Lung Adenocarcinoma. Ann Thorac Surg 2020;110:1036-1042.
6. Guo Q, Ke XX, Liu Z, et al. Evaluation of the Prognostic Value of STEAP1 in Lung Adenocarcinoma and Insights into Its Potential Molecular Pathways via Bioinformatic Analysis. Front Genet, 2020;11:242.
7. Cui D, Feng Y, Shi K, et al. Long non-coding RNA TRPM2-AS sponges microRNA-138-5p to activate epidermal growth factor receptor and PI3K/AKT signaling in non-small cell lung cancer. Ann Transl Med 2020;8:1313.
8. Li ZW, Zhang TY, Yue GJ, et al. Small nucleolar RNA host gene 22 (SNHG22) promotes the progression of esophageal squamous cell carcinoma by miR-429/SESN3 axis. Ann Transl Med 2020;8:1007.
9. Ke D, Guo Q, Fan TY, et al. Analysis of the Role and Regulation Mechanism of hsa-miR-147b in Lung Squamous Cell Carcinoma Based on The Cancer Genome Atlas Database. Cancer Biother Radiopharm 2021;36:280-91.
10. Xiao B, Zhang W, Chen L, et al. Analysis of the miRNA-mRNA-lncRNA network in human estrogen receptor-positive and estrogen receptor-negative breast cancer based on TCGA data. Gene 2018;658:28-35.
11. Yang J, Qiu Q, Qian X, et al. Long noncoding RNA LCAT1 functions as a ceRNA to regulate RAC1 function by sponging miR-4715-5p in lung cancer. Mol Cancer 2019;18:171.
12. Du LJ, Mao LJ, Jing RJ. Long noncoding RNA DNAH17-AS1 promotes tumorigenesis and metastasis of non-small cell lung cancer via regulating miR-877-5p/CCNA2 pathway. Biochem Biophys Res Commun 2020;533:565-72.
13. Zheng S, Zhou C, Wang Y, et al. TRIM6 promotes colorectal cancer cells proliferation and response to thiostrepton by TIS21/FoxM1. J Exp Clin Cancer Res 2020;39:23.
14. Wei C, Wu J, Liu W, et al. Tripartite motif-containing protein 6 facilitates growth and migration of breast cancer through degradation of STUB1. Eur J Histochem 2021;65:undefined.
15. Zhang H, Sun W, Qiao G, et al. The Expression of Tripartite Motif Protein 36 and β-Catenin Correlates with the Prognosis of Esophageal Cancer. Gastroenterol Res Pract 2020;2020:7641761.
16. Fang SX, Chen C, Guo Q, et al. High lncSNHG15 expression may predict poor cancer prognosis: a meta-analysis based on the PRISMA and the bio-informatics analysis. Biosci Rep 2020;40:BSR20194468.
17. Wang R, Wang X, Zhang J, et al. LINC00942 Promotes Tumor Proliferation and Metastasis in Lung Adenocarcinoma via FZD1 Upregulation. Technol Cancer Res Treat 2021;20:1533033820977526.
18. Huang Y, Zhong L, Nie K, et al. Identification of LINC00665-miR-let-7b-CCNA2 competing endogenous RNA network associated with prognosis of lung adenocarcinoma. Sci Rep 2021;11:4434.
19. Wang Y, Wo Y, Lu T, et al. Circ-AASDH functions as the progression of early stage lung adenocarcinoma by targeting miR-140-3p to activate E2F7 expression. Transl Lung Cancer Res 2021;10:57-70.
20. Pan LJ, Zhong TF, Tang RX, et al. Upregulation and clinicopathological significance of long non-coding NEAT1 RNA in NSCLC tissues. Asian Pac J Cancer Prev 2015;16:2851-5.
21. Zhou W, Chen X, Hu Q, et al. Galectin-3 activates

TLR4/NF-κB signaling to promote lung adenocarcinoma cell proliferation through activating lncRNA-NEAT1 expression. BMC Cancer 2018;18:580.
22. Zhang J, Li Y, Dong M, et al. Long non-coding RNA NEAT1 regulates E2F3 expression by competitively binding to miR-377 in non-small cell lung cancer. Oncol Lett 2017;14:4983-8.
23. Jen J, Tang YA, Lu YH, et al. Oct4 transcriptionally regulates the expression of long non-coding RNAs NEAT1 and MALAT1 to promote lung cancer progression. Mol Cancer 2017;16:104.
24. Sun C, Li S, Zhang F, et al. Long non-coding RNA NEAT1 promotes non-small cell lung cancer progression through regulation of miR-377-3p-E2F3 pathway. Oncotarget 2016;7:51784-814.
25. Li S, Yang J, Xia Y, et al. Long Noncoding RNA NEAT1 Promotes Proliferation and Invasion via Targeting miR-181a-5p in Non-Small Cell Lung Cancer. Oncol Res 2018;26:289-96.
26. Zhao L, Bi M, Zhang H, et al. Downregulation of NEAT1 Suppresses Cell Proliferation, Migration, and Invasion in NSCLC Via Sponging miR-153-3p. Cancer Biother Radiopharm 2020;35:362-70.
27. Xiong DD, Li ZY, Liang L, et al. The LncRNA NEAT1 Accelerates Lung Adenocarcinoma Deterioration and Binds to Mir-193a-3p as a Competitive Endogenous RNA. Cell Physiol Biochem 2018;48:905-18.
28. Li B, Gu W, Zhu X. NEAT1 mediates paclitaxel-resistance of non-small cell of lung cancer through activation of Akt/mTOR signalling pathway. J Drug Target 2019;27:1061-7.
29. Zang F, Rao Y, Zhu X, et al. Shikonin suppresses NEAT1 and Akt signaling in treating paclitaxel-resistant non-small cell of lung cancer. Mol Med 2020;26:28.
30. Mu L, Zhao H, Yang Y, et al. Long noncoding RNA NEAT1 aggravates sorafenib-resistance in non-small cell lung cancer via regulating miRNA-335/c-Met. J BUON 2021;26:345-52.
31. Zhang X, He X, Liu Y, et al. MiR-101-3p inhibits the growth and metastasis of non-small cell lung cancer through blocking PI3K/AKT signal pathway by targeting MALAT-1. Biomed Pharmacother 2017;93:1065-1073.
32. Du W, Tang H, Lei Z, et al. miR-335-5p inhibits TGF-β1-induced epithelial-mesenchymal transition in non-small cell lung cancer via ROCK1. Respir Res 2019; 20:225.
33. Yang H, Wang Z, Wang Z. Long Noncoding RNA KCNMB2-AS1 Increases ROCK1 Expression by Sponging microRNA-374a-3p to Facilitate the Progression of Non-Small-Cell Lung Cancer. Cancer Manag Res 2020;12:12679-12695.
34. Tanaka I, Dayde D, Tai MC, et al. SRGN-Triggered Aggressive and Immunosuppressive Phenotype in a Subset of TTF-1-Negative Lung Adenocarcinomas. J Natl Cancer Inst 2021;undefined:undefined..
35. Ma K, Qiao Y, Wang H, et al. Comparative expression analysis of PD-1, PD-L1, and CD8A in lung adenocarcinoma. Ann Transl Med 2020;8:1478.
36. Chen T, Chen J, Zhu Y, et al. CD163, a novel therapeutic target, regulates the proliferation and stemness of glioma cells via casein kinase 2. Oncogene 2019;38:1183-99.
37. Ma LL, Guo LL, Luo Y, et al. Cdc42 subcellular relocation in response to VEGF/NRP1 engagement is associated with the poor prognosis of colorectal cancer. Cell Death Dis 2020;11:171.
38. Vescarelli E, Gerini G, Megiorni F, et al. MiR-200c sensitizes Olaparib-resistant ovarian cancer cells by targeting Neuropilin 1. J Exp Clin Cancer Res 2020;39:3.

(English Language Editor: K. Brown)

Cite this article as: Ding DX, Li Q, Shi K, Li H, Guo Q, Zhang YQ. LncRNA NEAT1-miR-101-3p/miR-335-5p/miR-374a-3p/miR-628-5p-TRIM6 axis identified as the prognostic biomarker for lung adenocarcinoma via bioinformatics and meta-analysis. Transl Cancer Res 2021;10(11):4870-4883. doi: 10.21037/tcr-21-2181

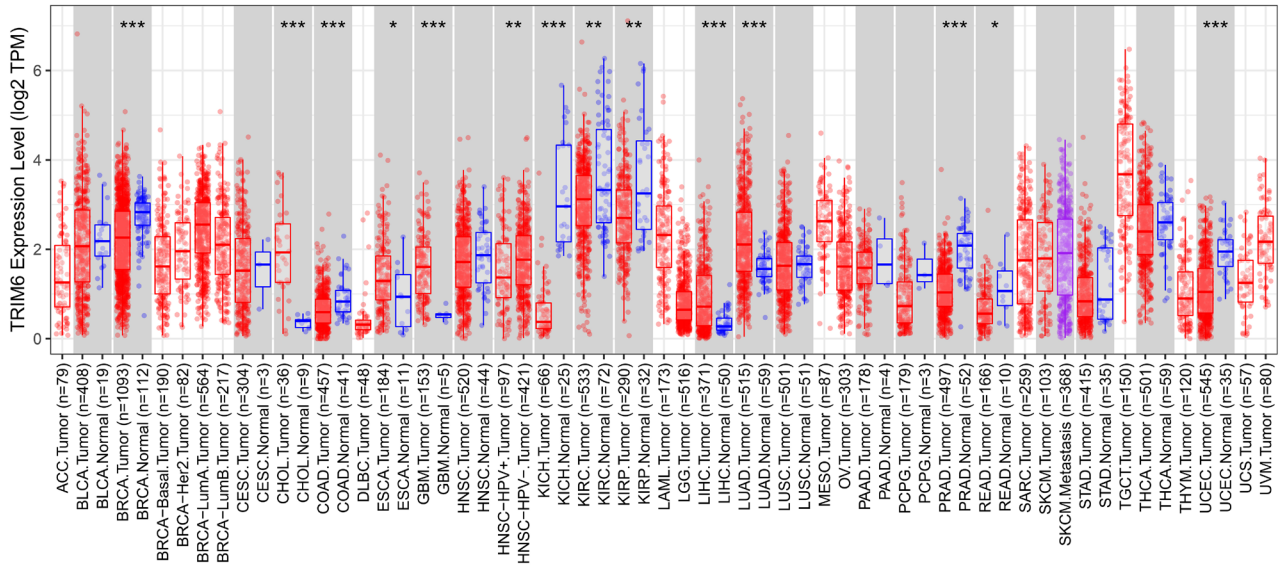

Figure S1 Abnormal expression of TRIM6 in pan-cancer tissues from the TIMER2 database. *, P<0.05; **, P<0.01; ***, P<0.001. TRIM6, tripartite motif containing 6.

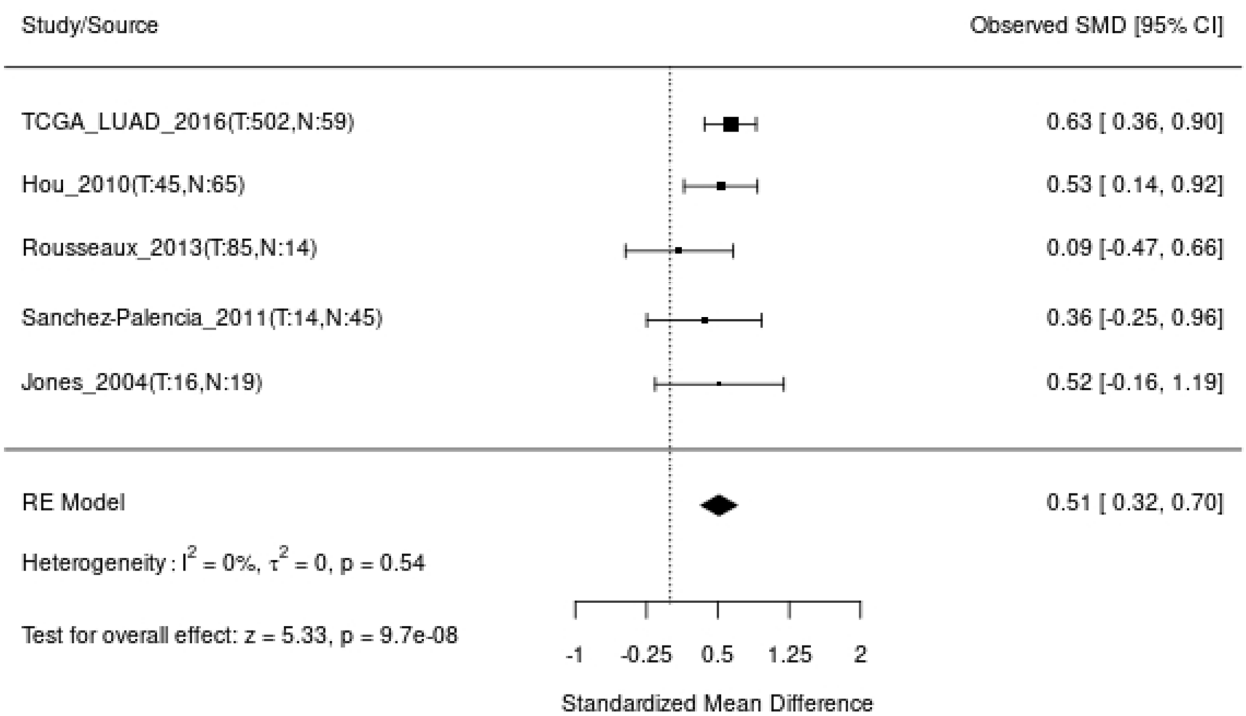

Figure S2 Overexpression of TRIM6 in LUAD tissues via meta-analysis. TRIM6, tripartite motif containing 6; LUAD, lung adenocarcinoma.

https://dx.doi.org/10.21037/tcr-21-2181

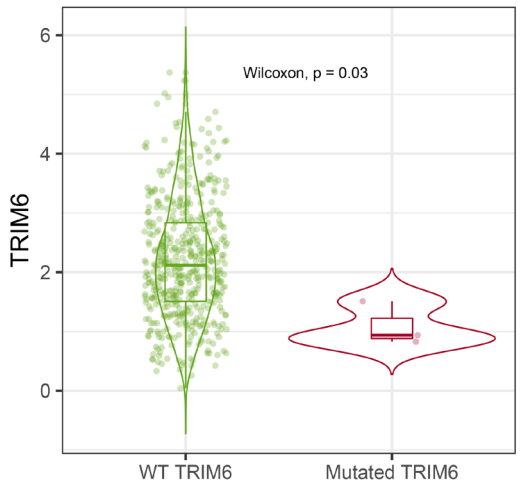

Figure S3 Statistical significance of TRIM6 expression level in wild- and mutant-types. TRIM6, tripartite motif containing 6.

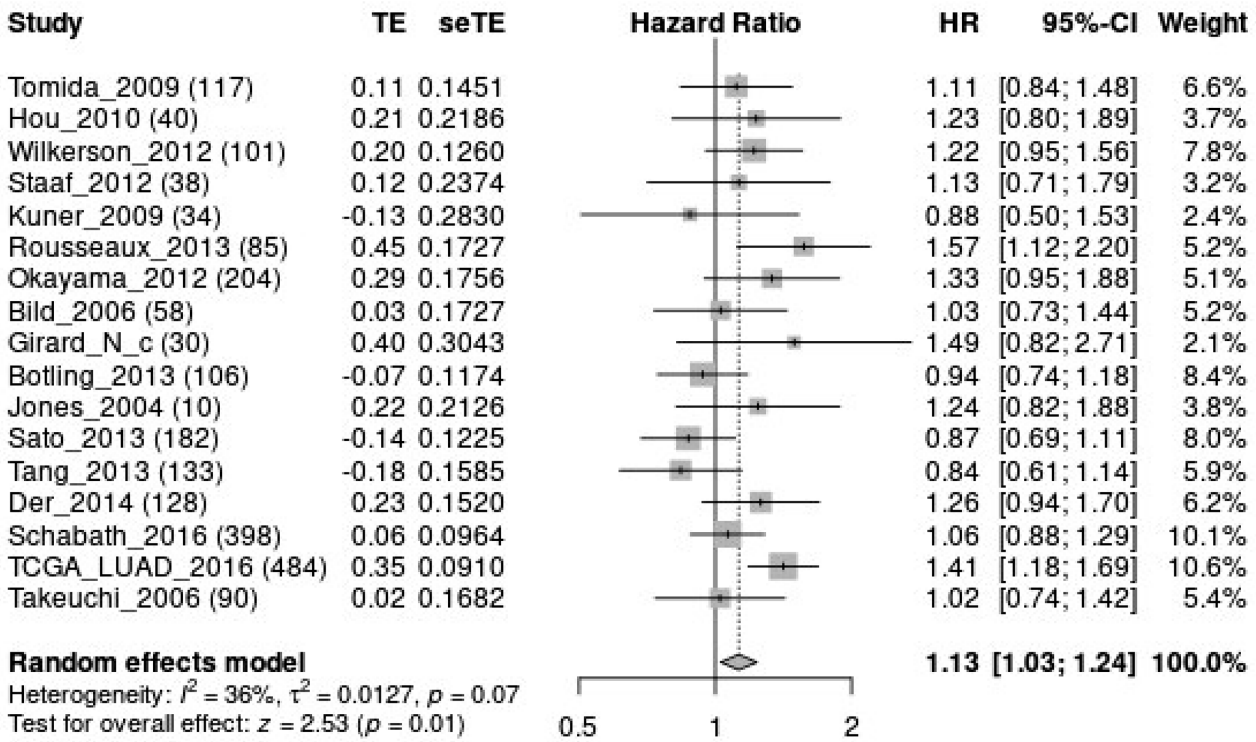

Figure S4 Association of TRIM6 overexpression with dismal prognosis in LUAD patients via meta-analysis. TRIM6, tripartite motif containing 6; LUAD, lung adenocarcinoma.

https://dx.doi.org/10.21037/tcr-21-2181

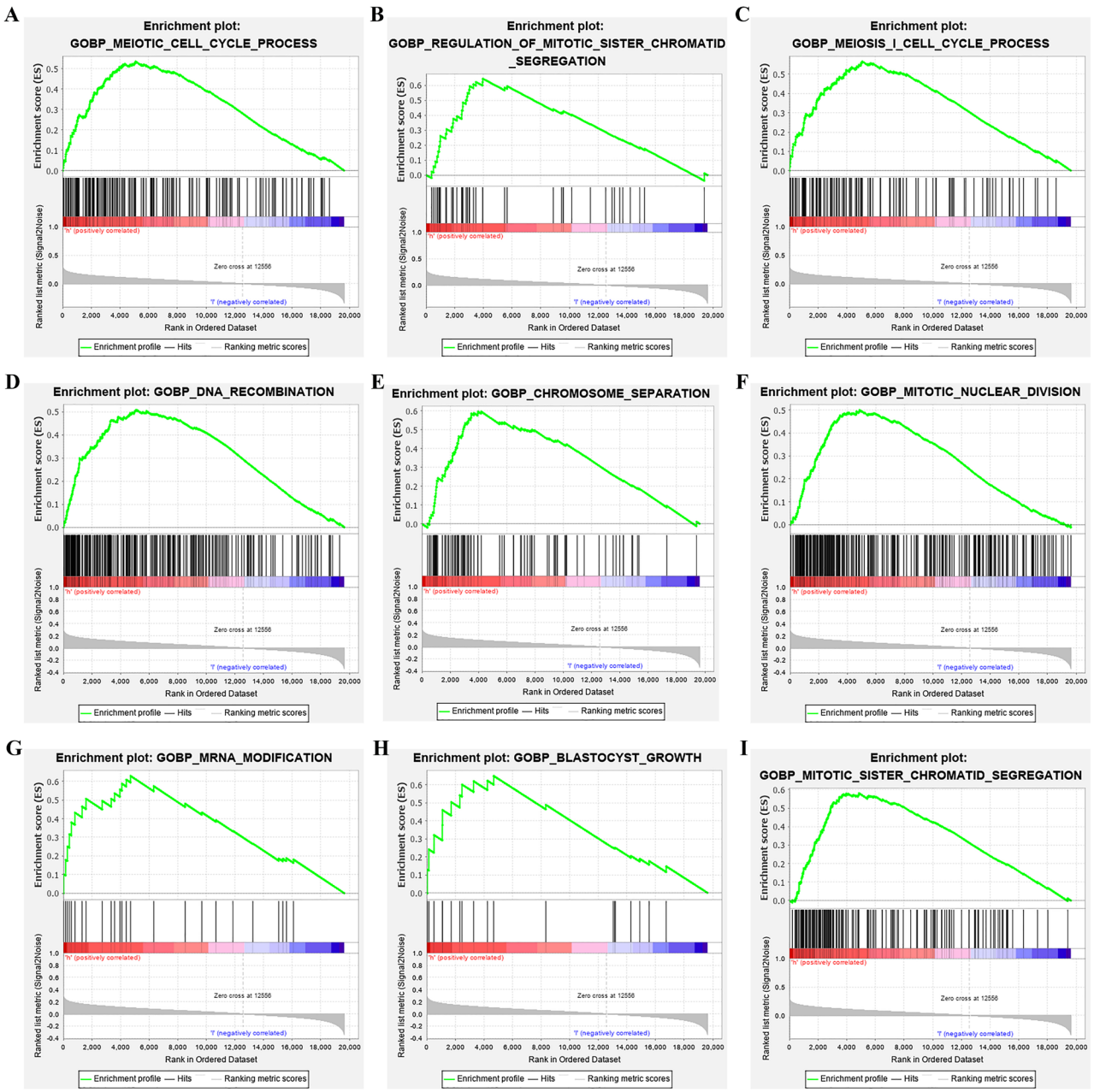

Figure S5 Possible involvement of TRIM6 in the biological functions of LUAD via gene set enrichment analysis. TRIM6, tripartite motif containing 6; LUAD, lung adenocarcinoma.

https://dx.doi.org/10.21037/tcr-21-2181

Table S1 Possible involvement of TRIM6 in the biological functions of LAC via gene set enrichment analysis

Type	Size	NES	NOM p
Protein polyubiquitination	328	2.0655742	0
Regulation of chromosome separation	69	2.0007765	0
Double strand break repair	248	1.989513	0.001949318
Chromosome separation	92	1.9889274	0.003816794
Recombinational repair	136	1.9847534	0
Positive regulation of defense response to virus by host	30	1.9818842	0
Meiotic cell cycle	242	1.9756027	0.001992032
Nuclear chromosome segregation	261	1.9673109	0.005882353
Chromosome segregation	323	1.9607008	0.005870841
Sister chromatid segregation	190	1.9484386	0.007858546
Meiosis I cell cycle process	121	1.9462405	0.002024292
Mitotic sister chromatid segregation	161	1.9437069	0.011627907
Replication fork processing	40	1.9385577	0.005882353
Metaphase anaphase transition of cell cycle	63	1.9362124	0.005836576
Telomere organization	146	1.936024	0
DNA recombination	277	1.9346648	0.007843138
DNA dependent DNA replication	157	1.932359	0.01171875
RNA methylation	80	1.9304466	0
Organelle fission	473	1.9303519	0.004016064
Meiotic cell cycle process	184	1.9299093	0.002028398
Regulation of mitotic sister chromatid segregation	44	1.9287176	0.007827789
Mitotic nuclear division	292	1.9174657	0.009689922
Meiotic chromosome segregation	85	1.9171549	0.00407332
Chromosome organization involved in meiotic cell cycle	64	1.9163623	0.002008032
Telomere maintenance via recombination	15	1.8963774	0
Regulation of chromosome segregation	84	1.8915232	0.007905139
Regulation of double strand break repair	84	1.8908021	0.003976143
DNA dependent DNA replication maintenance of fidelity	49	1.8879464	0.00996016
Regulation of defense response to virus	66	1.8852271	0
Regulation of telomere maintenance via telomere lengthening	60	1.8835573	0.002066116
DNA replication	279	1.8831266	0.01908397
Regulation of type I interferon mediated signaling pathway	34	1.8816944	0.004132231
SCF dependent proteasomal ubiquitin dependent protein catabolic process	92	1.8759762	0.00390625
Negative regulation of chromosome organization	88	1.8624744	0.00984252
Regulation of defense response to virus by host	40	1.8556365	0.002024292
Cellular response to ionizing radiation	64	1.8535588	0.002
Regulation of double strand break repair via nonhomologous end joining	28	1.851538	0.00203666
mRNA modification	25	1.8494092	0.003913894
Blastocyst growth	19	1.848844	0.004210526
Negative regulation of metaphase anaphase transition of cell cycle	41	1.8479091	0.019493178
Regulation of telomere maintenance	79	1.8467653	0.006160164
Regulation of transposition	26	1.8463326	0.004024145
Membrane disassembly	15	1.8456028	0.005976096
Mitotic recombination	24	1.840489	0.007889546
Postreplication repair	52	1.8396925	0.005859375
Sister chromatid cohesion	55	1.8393118	0
Negative regulation of nuclear division	54	1.8375087	0.01775148
Maintenance of protein location in nucleus	23	1.8354908	0.004246285
Oligosaccharide lipid intermediate biosynthetic process	21	1.8331665	0.001988072
Modulation by virus of host cellular process	18	1.8325902	0
Positive regulation of DNA replication	37	1.8324372	0.004032258
RNA modification	163	1.8277454	0.006122449
Homologous recombination	58	1.827212	0.008080808
DNA double strand break processing	25	1.824733	0.011881189
DNA geometric change	112	1.8239932	0.017578125
Cellular carbohydrate catabolic process	45	1.8213698	0
Homologous chromosome segregation	57	1.817825	0.006036217
Negative regulation of telomere maintenance via telomere lengthening	27	1.8165724	0.004016064
Regulation of mitotic nuclear division	109	1.815922	0.019762846
Protein modification by small protein removal	299	1.8151141	0
Interstrand cross link repair	56	1.8144042	0.00996016
Cellular response to virus	62	1.8094558	0
RNA 3 end processing	152	1.8071829	0.019607844
Positive regulation of telomere maintenance	51	1.8029904	0.008196721
Positive regulation of double strand break repair via nonhomologous end joining	16	1.8029343	0.00610998
Negative regulation of viral genome replication	50	1.793344	0.019305019
Regulation of viral genome replication	79	1.789701	0.009861933
mRNA methylation	16	1.788956	0.006060606
tRNA methylation	39	1.7867619	0.008196721
Nucleic acid phosphodiester bond hydrolysis	291	1.786635	0.005836576
Non recombinational repair	90	1.7844683	0.006048387
Regulation of stem cell differentiation	110	1.7821914	0.007827789
Response to ionizing radiation	139	1.7808094	0.004246285
Cell cycle g2 M phase transition	270	1.7789677	0.017441861
Positive regulation of double strand break repair	41	1.7763609	0.004056795
Telomere maintenance via telomere lengthening	79	1.7752088	0.010080645
Regulation of cell cycle g2 M phase transition	214	1.7729582	0.01764706
Transposition	31	1.772282	0.006024096
DNA replication independent nucleosome organization	38	1.771991	0.030360531
Positive regulation of chromosome separation	17	1.7672647	0.004008016
Polysaccharide catabolic process	27	1.7659845	0
Negative regulation of telomere maintenance	35	1.7628858	0.004065041
Cell cycle checkpoint	207	1.7625858	0.024291499
DNA dealkylation	34	1.7602825	0.008230452
Response to interferon beta	28	1.7585148	0.005940594
Nucleobase biosynthetic process	18	1.7528863	0.017892644
Regulation of protein polyubiquitination	23	1.7523298	0.00407332
snRNA processing	35	1.7519541	0.024856597
DNA synthesis involved in DNA repair	52	1.750701	0.011857707
Protein k48 linked ubiquitination	60	1.7494944	0.010526316
DNA conformation change	274	1.7472078	0.031434186
Nucleus organization	118	1.7452762	0.006355932
Translesion synthesis	42	1.7414287	0.01004016
Regulation of DNA recombination	93	1.7411702	0.016032064
Positive regulation of response to cytokine stimulus	56	1.7411567	0.010183299
Regulation of DNA dependent DNA replication	47	1.7345353	0.04892368
Protein k63 linked ubiquitination	56	1.7336906	0.006147541
Cytoskeleton dependent cytokinesis	85	1.7321087	0.012875536
Regulation of DNA replication	106	1.7296755	0.032128513
Histone phosphorylation	38	1.7291313	0.01629328
Glycosyl compound biosynthetic process	41	1.7280432	0.020283977
Regulation of DNA repair	127	1.7274215	0.015936255
Mitotic sister chromatid cohesion	26	1.7274014	0.008130081
Negative regulation of DNA repair	34	1.7263863	0.018036073
DNA strand elongation	26	1.7250932	0.015414258
Cytoplasmic pattern recognition receptor signaling pathway	71	1.7219815	0.00610998
Centromere complex assembly	40	1.7216959	0.03006012
Homologous chromosome pairing at meiosis	47	1.7216927	0.012121212
Mitotic cell cycle checkpoint	158	1.721513	0.033464566
Formation of extrachromosomal circular DNA	15	1.7201111	0.015748031
RNA dependent DNA biosynthetic process	69	1.7189876	0.01629328
Positive regulation of DNA templated transcription elongation	26	1.7167281	0.014112903
Mitotic cytokinesis	69	1.7158481	0.016666668
Negative regulation of telomere maintenance via telomerase	20	1.7155759	0.007889546
Cellular response to interferon beta	20	1.7134181	0.02366864
mRNA 3 end processing	99	1.7061754	0.03868472
Protein localization to chromosome	87	1.705618	0.033009708
Cytokinesis	158	1.703202	0.008602151
Nucleobase metabolic process	33	1.703117	0.022132797
fc epsilon receptor signaling pathway	111	1.7028207	0.016260162
Proteasomal protein catabolic process	474	1.7016457	0
Mismatch repair	33	1.7004143	0.028688524
Regulation of DNA templated transcription elongation	51	1.6986502	0.026422765
Positive regulation of organelle assembly	63	1.6985744	0.01026694
RNA polyadenylation	46	1.696868	0.029239766
Pyrimidine nucleobase metabolic process	16	1.6966265	0.021276595
Regulation of hematopoietic progenitor cell differentiation	89	1.6957196	0.015655577
Negative regulation of type i interferon production	44	1.6953702	0.018595042
Negative regulation of cell cycle g2 M phase transition	107	1.6935197	0.030947777
DNA unwinding involved in DNA replication	16	1.6928427	0.022
Pyrimidine containing compound biosynthetic process	38	1.6922145	0.02414487
Response to virus	345	1.6913255	0.008
Interleukin 1 mediated signaling pathway	100	1.6909347	0.02734375
DNA replication initiation	40	1.6889527	0.04347826
Cell cycle DNA replication	64	1.6882298	0.04733728
Macromolecule methylation	287	1.6861122	0.017928287
DNA methylation or demethylation	93	1.6852771	0.01
Mitotic spindle assembly	64	1.680707	0.042
DNA demethylation	28	1.6781073	0.016771488
Carbohydrate catabolic process	193	1.676927	0.00204499
Negative regulation of mitotic cell cycle	300	1.6752526	0.02357564
Regulation of mRNA catabolic process	210	1.6739118	0.020408163
ncRNA 3 end processing	49	1.6724991	0.029821074
Positive regulation of DNA repair	73	1.6717656	0.010162601
snRNA metabolic process	46	1.6713082	0.029296875
Regulation of nuclear division	134	1.6706567	0.043392505
Protein localization to kinetochore	19	1.6703609	0.036750484
Regulation of chromosome organization	265	1.670021	0.034
Centrosome duplication	71	1.6663222	0.027944112
Male meiotic nuclear division	46	1.6661023	0.010162601
Mitotic chromosome condensation	15	1.6654531	0.03868472
Negative regulation of cell cycle process	332	1.6620698	0.025641026
Regulation of mRNA 3 end processing	28	1.6617905	0.030303031
Toll like receptor 2 signaling pathway	17	1.6612055	0.040899795
Positive regulation of metaphase anaphase transition of cell cycle	15	1.6607779	0.01764706
Response to gamma radiation	51	1.6607736	0.014344262
Protein localization to cytoskeleton	58	1.6604872	0.018292682
Defense response to virus	254	1.6584971	0.014285714
Nucleoside metabolic process	102	1.6582175	0.0234375
tRNA modification	86	1.6577955	0.038539555
Positive regulation of telomere maintenance via telomere lengthening	36	1.6576422	0.026639344
Methylation	338	1.6567373	0.019723866
Chromosome localization	80	1.6555444	0.034
Regulation of transcription by RNA polymerase III	23	1.6554717	0.023076924
Pore complex assembly	20	1.6531744	0.031809144
Regulation of hematopoietic stem cell differentiation	74	1.6530024	0.034816246
g2 DNA damage checkpoint	35	1.6516953	0.03696498
Negative regulation of DNA dependent DNA replication	17	1.6509221	0.03846154
tRNA processing	124	1.6503595	0.03968254
Chromatin remodeling at centromere	31	1.6500474	0.0483559
snRNA transcription	75	1.646255	0.023904383
Microtubule organizing center organization	139	1.6456436	0.03258656
Regulation of signal transduction by p53 class mediator	175	1.6454203	0.03929273
Regulation of spindle assembly	25	1.6452734	0.018
Preassembly of gpi anchor in er membrane	17	1.6452149	0.022357723
Protein localization to chromosome centromeric region	25	1.6435722	0.04950495
Signal transduction by p53 class mediator	261	1.6434695	0.031007752
Pyrimidine containing compound catabolic process	39	1.6431837	0.020408163
Innate immune response activating signal transduction	117	1.6429831	0.027613413
Nuclear envelope organization	52	1.6416669	0.016460905
Regulation of response to DNA damage stimulus	216	1.6403896	0.016032064
Negative regulation of DNA recombination	33	1.6386507	0.031746034
Nuclear export	198	1.6379824	0.036
Nucleotide excision repair	107	1.636564	0.032193158
RNA localization	230	1.6360102	0.041420117
Type I interferon production	125	1.6354352	0.03629032
mRNA transport	148	1.6344478	0.04715128
Regulation of cell cycle phase transition	441	1.6341908	0.027131783
Spindle assembly	111	1.6336192	0.033864543
Positive regulation of peptidyl threonine phosphorylation	30	1.6331973	0.010526316
DNA integrity checkpoint	154	1.6325916	0.038854804
Glycosyl compound metabolic process	125	1.6321492	0.01775148
Telomere capping	40	1.6315233	0.01871102
Ribonucleoside metabolic process	70	1.6305566	0.027613413
Negative regulation of cell cycle phase transition	244	1.6303072	0.037181996
Regulation of viral life cycle	142	1.6290175	0.024340771
Nucleoside monophosphate metabolic process	72	1.6275378	0.025096525
Non canonical Wnt signaling pathway	153	1.626171	0.021113243
Regulation of mRNA metabolic process	334	1.6257578	0.03508772
Pyrimidine nucleoside biosynthetic process	16	1.6235046	0.03846154
mRNA cleavage	21	1.6228366	0.026915114
Entry of bacterium into host cell	15	1.6224107	0.049586777
Pyruvate metabolic process	149	1.6218556	0.014112903
RNA phosphodiester bond hydrolysis	151	1.6210061	0.02385686
Somatic diversification of immune receptors	72	1.6197379	0.029598309
Copper ion transport	16	1.6196064	0.016393442
Autophagosome organization	95	1.6186426	0.010660981
Positive regulation of leukocyte apoptotic process	26	1.6166025	0.01992032
NADH metabolic process	42	1.6161786	0.02970297
Regulation of double strand break repair via homologous recombination	46	1.6156191	0.046464648
Positive regulation of gene expression epigenetic	44	1.615551	0.030181086
Positive regulation of transcription initiation from RNA Polymerase II promoter	28	1.6155479	0.019607844
Nucleotide phosphorylation	131	1.61505	0.016064256
Centriole assembly	45	1.6147758	0.04637097
Spindle organization	178	1.6137023	0.04637097
Golgi organization	145	1.6119738	0.029288704
Stress granule assembly	23	1.6113374	0.03671706
Interferon beta production	50	1.6112705	0.030303031
Ribonucleoside monophosphate biosynthetic process	32	1.6110724	0.046511628
DNA templated transcription elongation	111	1.6100688	0.044265594
Regulation of DNA metabolic process	334	1.6090451	0.025896415
Lymphocyte homeostasis	56	1.6073787	0.040733196
Exit from mitosis	28	1.6067088	0.026209677
Ribonucleoside monophosphate metabolic process	54	1.6036354	0.02734375
Regulation of histone h3 k9 methylation	19	1.6015913	0.0392562
Viral genome replication	123	1.6010172	0.034068137
Protein k11 linked ubiquitination	29	1.6001047	0.02834008
Clathrin coat assembly	18	1.5998569	0.029469548
Base excision repair	39	1.5982872	0.036217302
ncRNA transcription	105	1.5977081	0.04133858
Activation of innate immune response	144	1.5942322	0.030487806
tRNA metabolic process	156	1.5940431	0.04950495
Protein localization to chromosome telomeric region	29	1.5926508	0.036960986
erad pathway	100	1.5913696	0.01775148
Nuclear transcribed mRNA catabolic process deadenylation dependent decay	76	1.5909041	0.030737706
Transcription by RNA polymerase I	60	1.5905643	0.047808766
Nucleotide sugar metabolic process	35	1.5892948	0.04233871
Membrane docking	180	1.5885885	0.016427105
Regulation of response to cytokine stimulus	170	1.5863873	0.022267206
Regulation of vacuole organization	47	1.5860375	0.019723866
Positive regulation of i kappab kinase NF kappab signaling	182	1.5859853	0.020408163
Purine nucleoside monophosphate metabolic process	41	1.5851974	0.03065134
Protein quality control for misfolded or incompletely synthesized proteins	28	1.5849327	0.04
Pyrimidine nucleoside metabolic process	36	1.5817347	0.04597701
Establishment of protein localization to telomere	18	1.5815899	0.04743083
rRNA methylation	25	1.580509	0.034764826
Protein localization to chromatin	25	1.5796822	0.04208417
Negative regulation of double strand break repair via homologous recombination	18	1.5793256	0.049407113
Dosage compensation	15	1.5769355	0.040511727
Regulation of sister chromatid cohesion	21	1.5737301	0.04140787
Regulation of biological process involved in symbiotic interaction	191	1.572002	0.028455285
Vesicle targeting	91	1.5716345	0.023605151
DNA modification	115	1.5715665	0.032128513
Nuclear transport	339	1.5706556	0.041257367
Regulation of cellular amide metabolic process	409	1.5695508	0.016194332
Protein monoubiquitination	64	1.5685945	0.041493777
Tumor necrosis factor mediated signaling pathway	169	1.5681828	0.041257367
Regulation of centrosome cycle	47	1.5681388	0.038617887
Nucleoside diphosphate metabolic process	154	1.5674165	0.014112903
rig i signaling pathway	25	1.5660802	0.032520324
Glutamine metabolic process	22	1.565387	0.046464648
Pyrimidine containing compound metabolic process	82	1.5637685	0.03168317
NAD metabolic process	50	1.5596288	0.034
Base conversion or substitution editing	20	1.5593028	0.042596348
Viral life cycle	339	1.5587832	0.016032064
Establishment of tissue polarity	123	1.5569111	0.033464566
Cytoplasmic pattern recognition receptor signaling pathway in response to virus	31	1.5560801	0.038306452
Positive regulation of response to DNA damage stimulus	106	1.5546569	0.030425964
Vacuole organization	170	1.5536447	0.006289308
Positive regulation of DNA metabolic process	197	1.553395	0.030181086
Guanosine containing compound metabolic process	39	1.5526001	0.016032064
Macroautophagy	306	1.5495206	0.01026694
Negative regulation of DNA metabolic process	109	1.5489824	0.046747968
Determination of adult lifespan	18	1.546193	0.04375
nik NF kappab signaling	167	1.5438156	0.043392505
Positive regulation of response to biotic stimulus	249	1.5433587	0.04897959
Regulation of spindle organization	39	1.540542	0.042769857
Regulation of exit from mitosis	16	1.5373284	0.048484847
Signal transduction in response to DNA damage	129	1.5361433	0.04715128
Viral RNA genome replication	33	1.5291849	0.034274194
Monosaccharide catabolic process	61	1.5286518	0.04761905
Post translational protein modification	358	1.5268416	0.007858546
Regulation of autophagosome assembly	38	1.5258355	0.038854804
DNA biosynthetic process	185	1.5239446	0.037848607
Regulation of translational initiation	80	1.5235577	0.038
Morphogenesis of a polarized epithelium	144	1.5226166	0.04296875
Regulation of carbohydrate catabolic process	88	1.5197762	0.04024145
Binding of sperm to zona pellucida	43	1.5171808	0.038986355
Protein localization to nucleus	273	1.5160446	0.016494846
Protein phosphopantetheinylation	329	1.5140212	0.008247423
Cellular response to gamma radiation	27	1.5138853	0.04660194
Positive regulation of translation	129	1.513046	0.042510122
Cellular response to heat	115	1.5113117	0.043209877
Pyridine containing compound metabolic process	41	1.5098954	0.023762377
Biological process involved in interaction with host	219	1.507992	0.018181818
Positive regulation of DNA templated transcription initiation	35	1.505726	0.047524754
Golgi vesicle transport	369	1.5033838	0.015250545
Regulation of organelle assembly	182	1.5015489	0.029787235
Tor signaling	116	1.5009478	0.023206752
DNA damage response signal transduction by p53 class mediator	105	1.4997541	0.034136545
Male meiosis I	23	1.4994725	0.033970278
Regulation of response to biotic stimulus	406	1.4925996	0.044989776
Nucleobase containing small molecule biosynthetic process	112	1.4857869	0.034136545
Protein import	193	1.4849188	0.03726708
Endomembrane system organization	468	1.476467	0.02783726
Regulation of tumor necrosis factor mediated signaling pathway	59	1.4691786	0.036659878
Endoplasmic reticulum organization	81	1.4663379	0.046709128
Response to heat	156	1.4625585	0.046558704
Phosphate ion transmembrane transport	15	1.461592	0.038229376
Maintenance of protein location in cell	64	1.4604704	0.031620555
Regulation of macroautophagy	158	1.4545101	0.029787235
Positive regulation of protein modification by small protein conjugation or removal	134	1.4407438	0.032258064
Establishment of organelle localization	425	1.4399235	0.03837953
Maintenance of protein localization in organelle	42	1.4307377	0.043912176
Regulation of autophagy	324	1.4213198	0.034408603
Female gamete generation	125	1.4089407	0.044989776
Negative regulation of oxidative stress induced cell death	40	1.4082843	0.045454547
Regulation of protein modification by small protein conjugation or removal	231	1.3988352	0.042168673
Maintenance of protein location	92	1.3823981	0.046938777
Cell death in response to oxidative stress	78	1.3608412	0.04595186
Regulation of proteasomal protein catabolic process	178	1.3602904	0.04809619

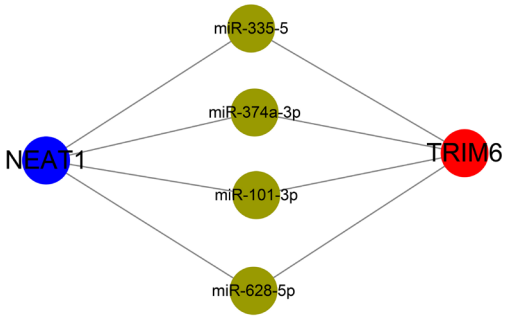

Figure S6 TRIM6 related-network.

https://dx.doi.org/10.21037/tcr-21-2181